Research Article | Vol. 26, No. 5 | 5 Mar 2018 | OPTICS EXPRESS 6260
Optics EXPRESS

High optical gain in erbium-doped potassium double tungstate channel waveguide amplifiers

SERGIO A. VÁZQUEZ-CÓRDOVA,[1] SHANMUGAM ARAVAZHI,[2] CHRISTOS GRIVAS,[3,4] YEAN-SHENG YONG,[1] SONIA M. GARCÍA-BLANCO,[1] JENNIFER L. HEREK,[1] AND MARKUS POLLNAU[2,5,*]

[1]*Optical Sciences Group, MESA + Institute for Nanotechnology, University of Twente, P.O. Box 217, 7500 AE Enschede, The Netherlands*
[2]*Integrated Optical Microsystems Group, MESA + Institute for Nanotechnology, University of Twente, P.O. Box 217, 7500 AE Enschede, The Netherlands*
[3]*School of Physics and Astronomy, University of Southampton, Southampton SO17 1BJ, UK*
[4]*Department of Applied Physics, KTH – Royal Institute of Technology, Stockholm SE-10691, Sweden*
[5]*Advanced Technology Institute, Department of Electrical and Electronic Engineering, University of Surrey, Guildford GU2 7XH, UK*
**m.pollnau@surrey.ac.uk*

Abstract: We report on the optical-gain properties of channel waveguides patterned into lattice-matched $KGd_xLu_yEr_{1-x-y}(WO_4)_2$ layers grown onto undoped $KY(WO_4)_2$ substrates by liquid phase epitaxy. A systematic investigation of gain is performed for five different Er^{3+} concentrations in the range of 0.75 to 10at.% and different pump powers and signal wavelengths. In pump-probe-beam experiments, relative internal gain, i.e., signal enhancement minus absorption loss of light propagating in the channel waveguide, is experimentally demonstrated, with a maximum value of 12 ± 5 dB/cm for signals at the peak-emission wavelength of 1534.7 nm.

© 2018 Optical Society of America under the terms of the OSA Open Access Publishing Agreement

OCIS codes: (130.0130) Integrated optics; (140.4480) Optical amplifiers; (160.5690) Rare-earth-doped materials.

References and links

1. J. D. B. Bradley and M. Pollnau, "Erbium-doped integrated waveguide amplifiers and lasers," Laser Photonics Rev. **5**(3), 368–403 (2011).
2. S. A. Vázquez-Córdova, M. Dijkstra, E. H. Bernhardi, F. Ay, K. Wörhoff, J. L. Herek, S. M. García-Blanco, and M. Pollnau, "Erbium-doped spiral amplifiers with 20 dB of net gain on silicon," Opt. Express **22**(21), 25993–26004 (2014).
3. K. Vu and S. Madden, "Tellurium dioxide erbium doped planar rib waveguide amplifiers with net gain and 2.8 dB/cm internal gain," Opt. Express **18**(18), 19192–19200 (2010).
4. J. Hoyo, V. Berdejo, T. T. Fernandez, A. Ferrer, A. Ruiz, J. A. Valles, M. A. Rebolledo, I. Ortega-Feliu, and J. Solis, "Femtosecond laser written 16.5 mm long glass-waveguide amplifier and laser with 5.2 $dBcm^{-1}$ internal gain at 1534 nm," Laser Phys. Lett. **10**(10), 105802 (2013).
5. R. Brinkmann, I. Baumann, M. Dinand, W. Sohler, and H. Suche, "Erbium-doped single- and double-pass Ti:$LiNbO_3$ waveguide amplifiers," IEEE J. Quantum Electron. **30**(10), 2356–2360 (1994).
6. L. Agazzi, K. Wörhoff, and M. Pollnau, "Energy-transfer-upconversion models, their applicability and breakdown in the presence of spectroscopically distinct ion classes: A case study in amorphous $Al_2O_3:Er^{3+}$," J. Phys. Chem. C **117**(13), 6759–6776 (2013).
7. J. Schmulovich, "Er-doped glass waveguide amplifiers on silicon," Proc. SPIE **2996**, 143–153 (1997).
8. P. G. Kik and A. Polman, "Cooperative upconversion as the gain-limiting factor in Er doped miniature Al_2O_3 optical waveguide amplifiers," J. Appl. Phys. **93**(9), 5008–5012 (2003).
9. F. D. Patel, S. DiCarolis, P. Lum, S. Venkatesh, and J. N. Miller, "A compact high-performance optical waveguide amplifier," IEEE Photonics Technol. Lett. **16**(12), 2607–2609 (2004).
10. G. Della Valle, S. Taccheo, P. Laporta, G. Sorbello, E. Cianci, and V. Foglietti, "Compact high gain erbium-ytterbium doped waveguide amplifier fabricated by Ag-Na ion exchange," Electron. Lett. **42**(11), 632–633 (2006).
11. J. D. B. Bradley, L. Agazzi, D. Geskus, F. Ay, K. Wörhoff, and M. Pollnau, "Gain bandwidth of 80 nm and 2 dB/cm peak gain in $Al_2O_3:Er^{3+}$ optical amplifiers on silicon," J. Opt. Soc. Am. B **27**(2), 187–196 (2010).

#322906 https://doi.org/10.1364/OE.26.006260
Journal © 2018 Received 9 Feb 2018; accepted 13 Feb 2018; published 28 Feb 2018

Optics EXPRESS

12. W.-B. Sun, X.-F. Yang, Z.-B. Zhang, W.-H. Wong, D.-Y. Yu, E. Y.-B. Pun, and D.-L. Zhang, "Optical damage resistant Ti-diffused Zr/Er-codoped lithium niobate strip waveguide for high-power 980 nm pumping," Opt. Express **25**(8), 8653–8658 (2017).
13. S. Suntsov, C. E. Rüter, and D. Kip, "Er:Ti:$LiNbO_3$ ridge waveguide optical amplifiers by optical grade dicing and three-side Er and Ti in-diffusion," Appl. Phys. B **123**(4), 118 (2017).
14. H. Sun, L. J. Yin, Z. C. Liu, Y. Z. Zheng, F. Fan, S. L. Zhao, X. Feng, Y. Z. Li, and C. Z. Ning, "Giant optical gain in a single-crystal erbium chloride silicate nanowire," Nat. Photonics **11**(9), 589–593 (2017).
15. D. Geskus, S. Aravazhi, S. M. García-Blanco, and M. Pollnau, "Giant optical gain in a rare-earth-ion-doped microstructure," Adv. Mater. **24**(10), OP19–OP22 (2012).
16. M. Pollnau, Y. E. Romanyuk, F. Gardillou, C. N. Borca, U. Griebner, S. Rivier, and V. Petrov, "Double tungstate lasers: from bulk toward on-chip integrated waveguide devices," IEEE J. Sel. Top. Quantum Electron. **13**(3), 661–671 (2007).
17. N. V. Kuleshov, A. A. Lagatsky, A. V. Podlipensky, V. P. Mikhailov, A. A. Kornienko, E. B. Dunina, S. Hartung, and G. Huber, "Fluorescence dynamics, excited-state absorption, and stimulated emission of Er^{3+} in $KY(WO_4)_2$," J. Opt. Soc. Am. B **15**(3), 1205–1212 (1998).
18. J. M. de Mendívil, G. Lifante, M. C. Pujol, M. Aguiló, F. Díaz, and E. Cantelar, "Judd-Ofelt analysis and transition probabilities of Er^{3+} doped $KY_{1-x-y}Gd_xLu_y(WO_4)_2$ crystals," J. Lumin. **165**, 153–158 (2015).
19. X. Mateos, R. Solé, J. Gavaldà, M. Aguiló, J. Massons, and F. Díaz, "Crystal growth, optical and spectroscopic characterisation of monoclinic $KY(WO_4)_2$ co-doped with Er^{3+} and Yb^{3+}," Opt. Mater. **28**(4), 423–431 (2006).
20. X. Mateos, M. C. Pujol, F. Guell, M. Galan, R. M. Sole, J. Gavalda, M. Aguiló, J. Massons, and F. Diaz, "Erbium spectroscopy and 1.5-µm emission in $KGd(WO_4)_2$:Er,Yb single crystals," IEEE J. Quantum Electron. **40**(6), 759–770 (2004).
21. M. C. Pujol, X. Mateos, R. Solé, J. Massons, J. Gavalda, X. Solans, F. Diaz, and M. Aguiló, "Structure, crystal growth and physical anisotropy of $KYb(WO_4)_2$, a new laser matrix," J. Appl. Cryst. **35**(1), 108–112 (2002).
22. I. M. Krygin, A. D. Prokhorov, V. P. D'yakonov, M. T. Borowiec, and H. Szymczak, "Spin-spin interaction of Dy^{3+} ions in $KY(WO_4)_2$," Phys. Solid State **44**(8), 1587–1596 (2002).
23. K. Petermann, D. Fagundes-Peters, J. Johannsen, M. Mond, V. Peters, J. J. Romero, S. Kutovoi, J. Speiser, and A. Giesen, "Highly Yb-doped oxides for thin-disc lasers," J. Cryst. Growth **275**(1–2), 135–140 (2005).
24. P. Loiko, S. J. Yoon, J. M. Serres, X. Mateos, S. J. Beecher, R. B. Birch, V. G. Savitski, A. J. Kemp, K. Yumashev, U. Griebner, V. Petrov, M. Aguiló, F. Díaz, and J. I. Mackenzie, "Temperature-dependent spectroscopy and microchip laser operation of Nd:$KGd(WO_4)_2$," Opt. Mater. **58**, 365–372 (2016).
25. F. Gardillou, Y. E. Romanyuk, C. N. Borca, R. P. Salathé, and M. Pollnau, "Lu, Gd codoped $KY(WO_4)_2$:Yb epitaxial layers: towards integrated optics based on $KY(WO_4)_2$," Opt. Lett. **32**(5), 488–490 (2007).
26. S. Aravazhi, D. Geskus, K. Van Dalfsen, S. A. Vázquez-Córdova, C. Grivas, U. Griebner, S. M. García-Blanco, and M. Pollnau, "Engineering lattice matching, doping level, and optical properties of $KY(WO_4)_2$:Gd, Lu, Yb layers for a cladding-side-pumped channel waveguide laser," Appl. Phys. B **111**(3), 433–446 (2013).
27. M. C. Pujol, M. Rico, C. Zaldo, R. Sole, V. Nikolov, X. Solans, M. Aguilo, and F. Diaz, "Crystalline structure and optical spectroscopy of Er^{3+}-doped $KGd(WO_4)_2$ single crystals," Appl. Phys. B **68**(2), 187–197 (1999).
28. M. C. Pujol, X. Mateos, A. Aznar, X. Solans, S. Suriñach, J. Massons, F. Díaz, and M. Aguiló, "Structural redetermination, thermal expansion and refractive indices of $KLu(WO_4)_2$," J. Appl. Cryst. **39**(2), 230–236 (2006).
29. T. Zayarnyuk, M. T. Borowiec, V. P. Dyakonov, H. Szymczak, E. Zubov, A. A. Pavlyuk, and M. Baranski, "Optical properties of potassium erbium double tungstate $KEr(WO_4)_2$," Proc. SPIE **4412**, 280–283 (2001).
30. R. Ulrich and R. Torge, "Measurement of thin film parameters with a prism coupler," Appl. Opt. **12**(12), 2901–2908 (1973).
31. D. Geskus, S. Aravazhi, C. Grivas, K. Wörhoff, and M. Pollnau, "Microstructured $KY(WO_4)_2$:Gd^{3+}, Lu^{3+}, Yb^{3+} channel waveguide laser," Opt. Express **18**(9), 8853–8858 (2010).
32. S. A. Vázquez-Córdova, S. Aravazhi, C. Grivas, A. M. Heuer, C. Kränkel, Y.-S. Yong, S. M. García-Blanco, J. L. Herek, and M. Pollnau, "Spectroscopy of erbium-doped potassium double tungstate waveguides," Proc. SPIE **10106**, 1010604 (2017).
33. D. Geskus, S. Aravazhi, K. Wörhoff, and M. Pollnau, "High-power, broadly tunable, and low-quantum-defect $KGd_{1-x}Lu_x(WO_4)_2$:Yb^{3+} channel waveguide lasers," Opt. Express **18**(25), 26107–26112 (2010).
34. K. van Dalfsen, S. Aravazhi, D. Geskus, K. Wörhoff, and M. Pollnau, "Efficient $KY_{1-x-y}Gd_xLu_y(WO_4)_2$:$Tm^{3+}$ channel waveguide lasers," Opt. Express **19**(6), 5277–5282 (2011).

1. Introduction

The great success of erbium-doped fiber amplifiers near 1.5 µm has triggered significant research on host materials and fabrication techniques for erbium-doped waveguide amplifiers (EDWA) [1–5]. Optical losses have limited the widespread application of integrated-optical circuit chips. The aim to compensate these losses has fueled the demand for on-chip-integrated host materials with erbium concentrations exceeding 10^{20} cm^{-3} to increase the gain in EDWAs. Low dopant solubility, which causes Er^{3+} clusters, is a major obstacle to increasing the erbium density in glass hosts. Furthermore, inter-ionic energy-transfer

Optics EXPRESS

processes are enhanced at increased erbium concentrations, thus limiting the maximum achievable gain [6].

In typical EDWAs gain per unit length of up to ~10 dB/cm has been reported so far [1,3–5,7–11]. With Yb co-doping, ~13 dB/cm were obtained [9]. Yb co-doping usually comes at the cost of lower total gain, because part of the pump power absorbed by Yb ions is followed by intrinsic decay rather than being transferred to Er ions. Erbium doped into crystalline materials has been the subject of recent investigations to increase the maximum achievable gain in waveguide amplifiers [12,13]. Recently, a gain of 100 dB/cm has been reported in a single-crystal erbium chloride silicate nanowire [14]. However, the fabrication method for such nanowires makes their integration in integrated photonic systems difficult and their dimension particularly complicates pump- and signal-light coupling.

A record-high optical gain of ~1000 dB/cm at 981 nm was demonstrated in an ytterbium-doped potassium double tungstate channel-waveguide amplifier [15]. In this family of host materials [16], rare-earth ions exhibit among the highest transition cross-sections reported so far [17–20], making these materials very promising for integrated amplifiers. Unlike in glass hosts, rare-earth ions in crystalline potassium double tungstates are located at significantly larger distances [21,22], thereby diminishing the probability of detrimental energy-transfer processes [23,24]. Due to the increased layer-substrate refractive index contrast by co-doping the layer with Gd and Lu ions [25,26], an improved field confinement in the guiding layer and large population inversion can be achieved in a potassium double tungstate channel-waveguide structure, resulting in high optical gain [15].

In this paper, we report on the fabrication and experimental characterization of optical gain in erbium-doped potassium gadolinium lutetium double tungstate, $KGd_xLu_yEr_{1-x-y}(WO_4)_2$, waveguide amplifiers. Five samples with Er^{3+} concentrations ranging from 0.75 to 10at.% are investigated. A relative internal gain of 12 ± 5 dB/cm at 1534.7 nm is demonstrated for an erbium concentration of 6at.% with a potentially exploitable bandwidth of ~116 nm.

2. Fabrication of channel waveguides

$KGd_xLu_yEr_{1-x-y}(WO_4)_2$ layers of high optical quality were grown onto laser-grade polished, 0.1 × 1 × 1 cm^3 large, 010-oriented, undoped $KY(WO_4)_2$ substrates by liquid phase epitaxy (LPE) [26] from high-purity (5N) raw materials (Alfa Aesar). An increased refractive-index contrast between the doped layer and the substrate of ~1.2×10^{-2} was achieved by substituting the Y^{3+} ions by optically inert Gd^{3+} and Lu^{3+} ions in the active layer. $KGd(WO_4)_2$ [27], $KLu(WO_4)_2$ [28], and $KEr(WO_4)_2$ [29] crystallize in the same monoclinic structure as $KY(WO_4)_2$. Whereas Gd^{3+} increases the lattice parameters, Lu^{3+} and Er^{3+} decrease it, such that appropriate fractions x and y of Gd^{3+} and Lu^{3+} ensure lattice matching with the $KY(WO_4)_2$ substrate for various Er^{3+} concentrations. Five samples with Er^{3+} concentrations ranging from 0.75 to 10at.% are studied and named Sample I-V (Table 1). Lapping and polishing of the layer surface parallel to the substrate-layer interface were performed to achieve the desired layer thickness and surface quality.

Refractive-index measurements were performed in sample III (see Table 1) using m-line spectroscopy [30] (Metricon 2010), with four different light sources with wavelengths at 0.633, 0.83, 1.3, and 1.55 µm. A least-squares fit of a single-term Sellmeier equation,

$$n_q^2 = 1 + B_q \lambda^2 / (\lambda^2 - C_q^2), \quad (1)$$

with $q = g, m, p$ representing the three axes of the optical indicatrix and λ the wavelength in units of µm, was performed, from which the Sellmeier coefficients were obtained (B_g = 3.187, C_g = 0.158, B_m = 2.999, C_m = 0.162, B_p = 2.879, and C_p = 0.158). All three refractive indices (n_g, n_m, and n_p) of the grown layers are in close agreement with those previously reported for similar layers doped with Yb^{3+} [26].

Optics EXPRESS

Rib channel waveguides parallel to the N_g axis in the N_m–N_g plane of the crystalline layer were micro-structured by Ar^+ etching [31], hence the optical modes could propagate with a polarization of either $E||N_m$ or $E||N_p$. Images of a patterned sample and an SEM image of the end facet of a channel waveguide are presented in Fig. 1. For all measurements, the signal and pump electric fields were aligned parallel to the N_m axis, i.e., with transverse-electric (TE) polarization. Composition (nominal values of the initial solution with an accuracy of 10^{-3}at.% [26]) and channel dimensions such as polished-layer thickness (t), etch depth (d), channel width (w), and length (ℓ) of each investigated sample are given in Table 1. Channels support the zero-order and first-order modes at pump and signal wavelengths for TE polarization.

Fabrication defects in channel waveguides appeared after patterning of all samples. These defects, ranging in size from a couple to hundreds of micrometers in length, were introduced during the lithographic process, presumably caused during manipulation or contact with the photoresist after exposure. These defects were transferred to the guiding layer during the ion-beam etching. Samples I, II, and III had continuous channel waveguides without defects across the initial sample length (≥ 8 mm), whereas samples IV and V suffered from large defects truncating the channel waveguides, which lead to strong scattering of the coupled light at each defect position. Consequently, the samples were diced into smaller sections where no disruptions in the channel waveguides were observed.

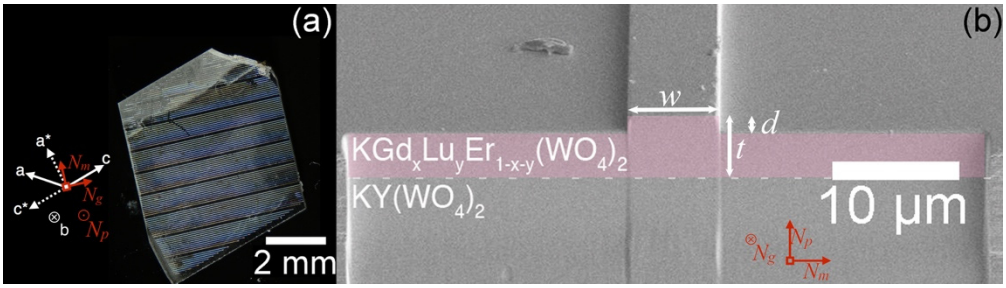

Fig. 1. (a) Channel waveguides in a latticed-matched $KGd_{0.489}Lu_{0.495}Er_{0.015}(WO_4)_2$ layer (sample II). Both the crystallographic axes and the axes of the optical indicatrix are indicated. (b) SEM image of the end facet of a channel waveguide showing the different cross-section parameters (i.e., w, t and d). The doped/guiding region is highlighted in pink color. The axes of the optical indicatrix are indicated.

Table 1. Parameters of the samples studied in this work: dopant concentrations, waveguide dimensions, overlap between pump profile and doped waveguide region, and measured relative internal gain per unit length achieved in gain saturation.

Sample	Lu^{3+}	Gd^{3+}	Er^{3+} (N_d)		t	w	d	ℓ	Γ	γ–$\alpha_{abs,S}$
	at.%	at.%	at.%	cm^{-3}	[μm]	[μm]	[μm]	[mm]		[dB/cm]
I	49.23	50.02	0.75	0.48 ×	6.4	5.6	1.48	5.07	0.93	1.96
II	48.96	49.55	1.50	0.95 ×	7.7	7.9	1.43	8.60	0.96	4.16
III	48.50	48.50	3.00	1.90 ×	7.1	7.8	1.27	6.75	0.95	7.95
IV	47.56	46.44	6.00	3.81 ×	8.5	7.5	1.55	0.75	0.97	12.09
V	46.26	43.74	10.00	6.36 ×	3.1	5.6	1.56	0.58	0.64	10.25

3. Gain characterization

Measurements of signal enhancement were performed in a free-space pump-probe setup, consisting of a continuous-wave Ti:Sapphire laser as the pump source on the $^4I_{15/2} \rightarrow {}^4I_{11/2}$ ground-state-absorption (GSA) transition and a laser diode (Agilent 81600B) as the signal source on the $^4I_{13/2} \rightarrow {}^4I_{15/2}$ gain transition, modulated at 1 kHz for lock-in detection. The incident signal power was set below 1 μW, such that the gain measurements were performed in the small-signal-gain regime. The pump wavelength was centered at 984.5 nm, because

Optics EXPRESS

pump excited-state absorption (ESA) on the $^4I_{11/2} \rightarrow {}^4F_{7/2}$ transition is weaker at this wavelength compared to shorter wavelengths, whereas only a small penalization in the GSA cross-section is encountered [32]. The pump and signal beams were combined by use of a dichroic mirror and launched into the channel waveguide by a × 10 microscope objective. At the output side, the amplified signal and residual pump were collimated using a × 60 microscope objective. The residual pump was attenuated using a 3 mm thick Silicon filter, whereas the transmitted signal was coupled through a multimode fiber into a monochromator (H25 Yvon Jobin), where the amplified spontaneous emission (ASE) and signal were dispersed, and detected by a InGaAs detector connected to a lock-in-amplifier. The combination of the Si filter, the monochromator, and the lock-in amplifier suppressed any contribution of residual pump and ASE to the signal-enhancement measurement.

The internal signal enhancement per unit length in dB/cm is given by,

$$\gamma = \frac{10}{\ell} \log_{10}\left[P_{S,P_{P,on}} / P_{S,P_{P,off}} \right] \tag{2}$$

where $P_{S,Pp,on}$ and $P_{S,Pp,off}$ are the transmitted signal power when the channel is pumped and unpumped, respectively. It was determined directly from the measured results of the pump-probe experiment. The relative internal gain ($\gamma - \alpha_{abs,S}$) was then obtained by subtracting the calculated Er^{3+} absorption coefficient of the unpumped sample at the signal wavelength of 1534.7 nm given by $\alpha_{abs,S} = 10 \log_{10}(e^1)\ \sigma_{a,S}\ N_d\ \Gamma$ (in dB/cm), where $\sigma_{a,S}$ is the absorption cross-section of Er^{3+} in the host crystal at the signal wavelength (1534.7 nm), N_d is the dopant concentration of each sample, and Γ is the calculated overlap factor of the signal-mode profile with the doped region. The values of Γ and N_d are given in Table 1. A value of 2.51×10^{-20} cm^2 was used for $\sigma_{a,S}$ [17].

The air-cladded channel waveguides investigated here exhibited rather high propagation losses of $\alpha_{loss} > 1$ dB/cm, compared to typical propagation losses α_{loss} found in buried channel waveguides ranging from 0.34 dB/cm near 1 μm [33] down to 0.11 dB/cm near 1.8 μm [34] due to the increased sidewall scattering at the double tungstate/air interface. Furthermore, the propagation losses varied significantly from sample to sample because of the above-mentioned individual fabrication errors. For the sake of meaningful comparison between the different dopant concentrations, as well as to highlight the potential of erbium-doped channel waveguides in this material, only the relative internal gain ($\gamma - \alpha_{abs,S}$) is reported. However, the internal net gain achievable for different propagation losses can be obtained in first-order approximation, i.e., neglecting the effect of pump reduction along the length of the amplifier due to the propagation losses, from the values in Table 1 by subtracting the propagation loss in dB/cm.

Figure 2(a) displays the experimental relative internal gain at 1534.7 nm as a function of incident pump power for the set of samples. For sample IV, for which $\alpha_{abs,S} = 40.83$ dB/cm, a maximum internal gain of ~12 ± 5 dB/cm was experimentally achieved for an incident pump power of ~600 mW.

The maximum relative internal gain values measured at 1534.7 nm for the complete set of five samples are presented in Fig. 2(b). For each sample, the internal gain as a function of incident pump power was measured. The maximum relative internal gain plotted in Fig. 2(b) is the value at saturation. For the pump powers utilized in these measurements, the five samples operated under gain saturation. Therefore, the values of gain per unit length presented in Fig. 2(b) can be directly compared to each other. For the given waveguide geometries, the maximum gain per unit length is achieved at a doping concentration of 3.8×10^{20} cm^{-3} (sample IV). In Fig. 2(b) it can be seen that the maximum achievable gain per unit length is reduced for the highest doping concentration. Detrimental effects, including energy-transfer upconversion (ETU) and pump excited-state absorption (ESA) are responsible for the decrease of gain at increasing Er^{3+} concentrations [6,8,32].

Optics EXPRESS

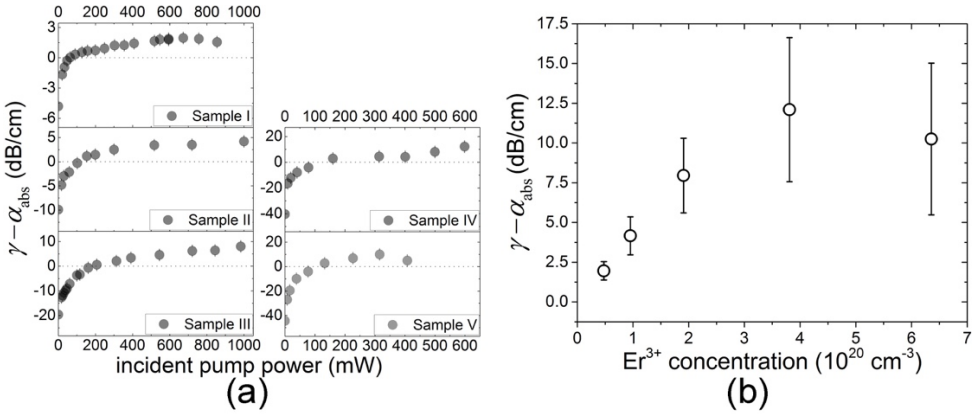

Fig. 2. (a) Relative internal gain, i.e., signal enhancement minus absorption loss, at λ_S = 1534.7 nm in a range of pump powers for the set of five samples. (b) Experimental relative internal gain at λ_S = 1534.7 nm at the pump power required to achieve gain saturation, for the range of Er^{3+} concentrations studied in this work.

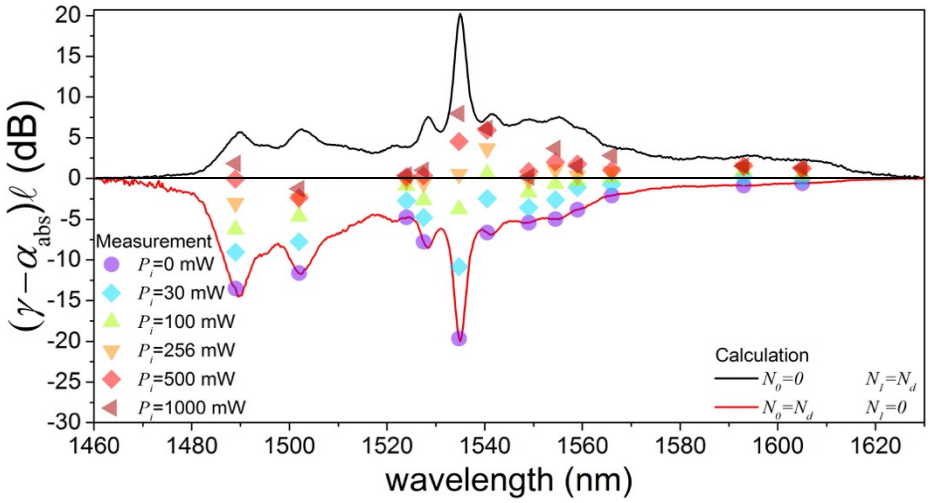

Fig. 3. Calculated (curves) and measured (data points) values of total internal gain in sample III as a function of signal wavelength for different incident pump powers.

Wavelength-dependent total relative internal gain in dB was measured from 1489 nm to 1605 nm in sample III (Fig. 3). Signal-enhancement measurements, at the complete emission spectrum, were the highest for sample III due to its combination of large waveguide length and relatively high doping concentration. Therefore, sample III was selected for the wavelength-dependent gain measurement. The total relative internal gain for different incident pump powers was determined across the spectral range (data points in Fig. 3). From Fig. 3, an internal gain bandwidth (defined between the two points of $\gamma-\alpha_{abs,S}$ = 0 dB) of 116 nm could be obtained for > 500 mW of incident pump power. The bottom and top curves in Fig. 3 represent the wavelength-dependent relative internal gain for zero and complete excitation of the $^4I_{13/2}$ amplifier level, calculated as the absorption cross section [17] multiplied by $N_0 = N_d$ and the emission cross section [17] multiplied by $N_1 = N_d$, respectively. From the data points in Fig. 3, it is possible to see that, as the pump power is increased, the signal absorption reduces until positive relative internal gain can be observed. A lower threshold for longer wavelengths is observed for incident powers ~256 mW. Amplification further extends to the blue-side of the spectrum as the excitation density of the $^4I_{13/2}$ level, N_1,

Optics EXPRESS

is increased by rising the pump power. Positive relative internal gain was measured in a wide range of the spectrum covering not only the C-band but also partially the S and L bands. This displays the great potential of the erbium-doped potassium double tungstates in a waveguide structure for broadband amplification.

4. Summary

A maximum relative internal gain of 12 ± 5 dB/cm at the signal wavelength of 1534.7 nm was demonstrated in Er^{3+}-doped potassium double tungstate channel waveguides. A gain bandwidth of ~116 nm has been shown for incident pump powers of >500 mW.

Funding

Dutch Technology Foundation (STW) (11689); National Science and Technology Council of Mexico (CONACyT) (scholarships abroad).

Acknowledgment

The authors gratefully acknowledge the great support of Meindert Dijkstra and Frans Segerink in the preparation of the samples.

152.78.210.55 (to 2018-04-09 08:13:44)